Diffusion-weighted MRI for detection and differentiation of musculoskeletal tumorous and tumor-like lesions in pediatric patients

Henning Neubauer, Laura Evangelista, Nicole Hassold, Beate Winkler, Paul Gerhardt Schlegel, Herbert Köstler, Dietbert Hahn, Meinrad Beer
Wuerzburg, Germany

Background: MRI is the diagnostic mainstay for detection and differentiation of musculoskeletal tumors. However, a projection regarding the biological dignity of lesions based on standard MRI sequences remains difficult and uncertain. This study was undertaken to analyse whether diffusion-weighted MRI (DWI) can distinguish between benign and malignant musculoskeletal tumorous and tumor-like lesions in pediatric patients.

Methods: MR examinations of 44 consecutive pediatric patients (26 girls, mean age 11±6 years) including standard sequences and DWI (b=50/800 s/mm^2) at 1.5 or 3 Tesla were retrospectively evaluated. The study group contained 10 patients with non-treated malignant tumors and 34 patients with benign lesions. Size, relative signal intensity and apparent diffusion coefficient (ADC, unit ×10^{-3} mm^2/s) were determined in one lesion per patient.

Results: Mean ADC was 0.78±0.45×10^{-3} mm^2/s in patients with malignant tumors and 1.71±0.75 ×10^{-3} mm^2/s in patients with benign lesions (*P*<0.001). Relative operating characteristics (ROC) analysis showed a sensitivity of 90% and a specificity of 91% for malignancy, based on an ADC cut-off value of ≤1.03. On logistic regression, mean ADC and lesion size accounted for 62% of variability in benign *vs.* malignant tumors. For malignant tumors, the signal intensity ratio was higher on DWI than on T1w post-contrast images (*P*<0.002). Two cases of local tumor recurrence were diagnosed by DWI only.

Conclusions: DWI shows promising results for determination of biological dignity in musculoskeletal tumors. Mean ADC ≤1.03×10^{-3} mm^2/s is a strong indicator of malignancy at the first diagnosis. The use of DWI for early diagnosis of tumor recurrence in comparison with standard MRI sequences should be evaluated in prospective studies.

Author Affiliations: Department of Pediatric Radiology, Institute of Radiology, University of Wuerzburg, Josef-Schneider-Straße 2, Wuerzburg 97080, Germany (Neubauer H, Evangelista L, Hassold N, Beer M); Department of Pediatrics, University of Wuerzburg, Josef-Schneider-Straße 2, Wuerzburg 97080, Germany (Winkler B, Schlegel PG); Institute of Radiology, University of Wuerzburg, Oberduerrbacher Str. 6, Wuerzburg 97080, Germany (Koestler H, Hahn D).

Corresponding Author: Henning Neubauer, MD, MBA, Department of Pediatric Radiology, Institute of Radiology, University Hospital Wuerzburg, Josef-Schneider-Straße 2, Wuerzburg 97080, Germany (Tel: 0049-931-201-34715; Fax: 0049-931-201-34857; Email: neubauer@roentgen.uni-wuerzburg.de).

Introduction

Soft tissue masses and osseous lesions are commonly encountered in pediatric patients. Although benign in most cases, a significant proportion constitutes malignant tumors.[1] The ability to differentiate benign from malignant disease is limited clinically. Therefore, multimodal diagnostic imaging plays an essential role in determining dignity, stratifying risk and guiding biopsy.[2] Magnetic resonance imaging (MRI) is an established modality for comprehensive diagnosis of musculoskeletal tumors, particularly in pediatric patients. However, data on diagnostic accuracy of MRI in predicting dignity of musculoskeletal tumors vary widely in the literature. Some studies[1,3,4] reported high sensitivity and specificity, while others stressed the non-specific appearance of most lesions.[5] In addition, there is a general paucity of prospective data from pediatric patients.

Diffusion-weighted imaging (DWI) has been introduced as a novel sequence for extra-neurological imaging. Available data, mostly from adult patients, have shown improved detection of pathological lesions and

an interesting potential for tissue characterization based on altered diffusivity of free water in inflammatory and neoplastic foci.[6] DWI of musculoskeletal lesions has been a major focus of ongoing research[7-9] and has shown promising results in therapy surveillance of primary malignant bone tumors.[10,11] To date, the diagnostic use of DWI in differentiating common musculoskeletal tumors and tumor-like lesions has not yet been subjected to systematic evaluation in pediatric patients. We therefore studied a series of consecutive pediatric patients with musculoskeletal tumors and tumor-like lesions so as to assess the feasibility of diffusion-weighted MRI in children, to compare findings on DWI with those on standard MRI, and to analyze the use of DWI in predicting tumor dignity.

Methods

This study included 44 consecutive patients (26 girls) with a mean age of 11±6 years (range 4 weeks to 19 years) who had been examined in a 3-year period. The study was conducted in accordance with the principles of *Helsinki Declaration*. Since it was a retrospective analysis of data from routine imaging studies, the approval from the institutional review board was not necessary. The treatment contract between patients and our university hospital covers the use of anonymous imaging data for scientific purposes. Informed written consent was obtained from the legal guardians of all patients for all diagnostic and therapeutic measures.

The study group included 10 patients with non-treated malignant tumors and 34 patients with benign tumors or tumor-like lesions (Table 1). All malignancies were confirmed by surgical biopsy or histology. Histological correlation was available in 16 of the 34 patients with benign lesions. In the remaining patients, multimodal imaging, follow-up imaging or both showed typical findings of benign lesions, so that no biopsy was performed.

MRI was performed routinely on 1.5 Tesla (Magnetom Symphony, *n*=24 and Magnetom Avanto, *n*=16) and 3 Tesla (Magnetom Skyra, *n*=3 and

Magnetom Trio, *n*=1) scanners. Twelve patients aged 4 weeks to 6 years required sedation. In addition to T1w and T2w imaging and contrast-enhanced sequences, we obtained regional transversal diffusion-weighted images by single-shot echo-planar imaging (SS-DW-EPI) and with free-breathing technique. DWI scans were performed before the application of intravenous contrast medium with a b-value of 50/800 s/mm^2, an orthogonal 3-scan-trace technique, and phase partial Fourier 6/8. Detailed information on DWI protocols is shown in Table 2. We used DWI with a large FOV and a scan volume for lesions located at the trunk and DWI with a small FOV and a targeted scan volume for the head/neck and extremities as well as the trunk of young patients.

Table 1. Description of musculoskeletal lesions in the study group

	Malignant tumors (*n*=10)	Benign tumors and tumor-like lesions (*n*=34)
Lesion entity	Ewing sarcoma, *n*=3	Hemangioma, *n*=6
	Osteosarcoma	Non-ossifying fibroma, *n*=5
	Desmoplastic small round cell tumor	Lymphangioma, *n*=4
	Primitive myxoid sarcoma	Arteriovenous malformation, *n*=3
	Local recurrence of alveolar rhabdomyosarcoma	Osteochondroma, *n*=2
	Local recurrence of synovial sarcoma	Epidermoid, *n*=2
	Osseous metastasis of neuroblastoma	Langerhans cell histocytosis, *n*=2
	Metastasis of adrenocortical carcinoma	Benign desmoid tumor
		Desmoid fibromatosis
		Inflammatory soft tissue tumor
		Osteoidosteoma
		Aneurysmatic bone cyst
		Fibrous dysplasia
		Neurofibroma
		Schwannoma
		Ameloblastic fibro-odontoma
		Benign myofibroblastic soft tissue tumor
Lesion localization	Head, *n*=1; trunk, *n*=5; neck, *n*=2; extremities, *n*=2	Head, *n*=10; trunk, *n*=1; neck, *n*=5; extremities, *n*=18
Lesion diameter	40±21 mm	23±14 mm
ROI size	1.88±0.89 cm^2	1.73±0.94 cm^2
Lesion ADC	0.78±0.45×10^{-3} mm^2/s	1.72±0.75×10^{-3} mm^2/s

ADC: apparent diffusion coefficient; ROI: region of interest.

Table 2. DWI sequence parameters implemented on different scanner hardware and the number of patients examined with each protocol

1.5 Tesla Magnetom Symphony	Large FOV, *n*=8	TR 9000 ms, TE 126 ms, flip angle 90°, bandwidth 1056 Hz/pixel, 8 averages, epi factor 128, FOV 360, voxel size 2.8×2.8×6.0 mm^3, 40 slices, scan time 7 min 21 s
	Small FOV, *n*=16	TR 4600 ms, TE 137 ms, flip angle 90°, bandwidth 1056 Hz/pixel, 2 to 6 averages, epi factor 128, FOV 230, voxel size 1.8×1.8×6.0 mm^3, 19 slices, scan time 41 s to 2 min 55 s
1.5 Tesla Magnetom Avanto	*n*=16	TR 5800 ms, TE 89 ms, flip angle 90°, bandwidth 1532 Hz/pixel, 8 averages, epi factor 192, GRAPPA acceleration factor 2, FOV 360, voxel size 1.9×1.9×6.0 mm^3, 40 slices, scan time 4 min 56 s
3 Tesla Magnetom Skyra	*n*=3	TR 3000 ms, TE 68 ms, flip angle 90°, bandwidth 1180 Hz/pixel, 8 averages, epi factor 94, GRAPPA acceleration factor 2, FOV 150, voxel size 1.4×1.4×6.0 mm^3, 15 slices, scan time 3 min 27 s
3 Tesla Magnetom Trio	*n*=1	TR 5100 ms, TE 73 ms, flip angle 90°, bandwidth 1736 Hz/pixel, 5 averages, epi factor 115, GRAPPA acceleration factor 2, FOV 380, voxel size 2.5×2.0×5.0 mm^3, 30 slices, scan time 4 min 23 s

DWI: diffusion-weighted imaging; FOV: field of view.

Isotropically diffusion-weighted images obtained at high b-values and contrast-enhanced T1w (ce-T1w) images were used for lesion detection and for measurement of signal intensity and largest transversal diameter. The total apparent diffusion coefficient (ADC_{total} 80/500) was quantitatively measured with a circular region of interest (ROI) on automatically generated ADC maps measuring a representative portion of one lesion per patient. We recorded minimum, maximum and mean ADC. In small lesions up to 15 mm in diameter, ROI diameter was equal to the minimum transversal diameter of the tumor, whereas in large lesions we measured ROIs of 10-20 mm in diameter, preferably in those regions exhibiting restricted diffusion (Table 1).

Mean ADC of pontine brain tissue, bulbus oculi, skeletal muscle and cerebrospinal fluid (CSF) were measured as internal reference if they were included in the scan volume. Lesion detection was performed by two experienced observers in consensus. All quantitative analyses were performed by one board-certified radiologist with 3 years of experience in extra-cranial DWI, who was blinded to clinical information. Signal intensity ratios were computed as mean signal intensity of the lesion divided by the mean signal intensity of surrounding normal bone marrow or soft tissue.

Statistical analysis

Normally distributed data are presented as mean± standard deviation. Between-groups comparison was made with the independent sample t test or the paired sample t test for variables following normal distribution. Wilcoxon's rank-sum test was used for between-groups comparison of signal intensity ratios, which deviated from normal distribution. Bivariate correlation analysis was employed to study the association between ADC and tumor size. The sensitivity and specificity of ADC measurements were studied with receiver operating characteristic (ROC) analysis. Regression analysis based on a binary logistic regression model with tumor dignity as the dependent variable was established to analyse the association between tumor size, ADC and dignity. P value <0.05 was considered statistically significant. Analyses were made with the PASW (SPSS) Statistics 18 software for Windows.

Results
Feasibility
All MRI examinations were completed in accordance with the scan protocol. The additional scanning time for DWI
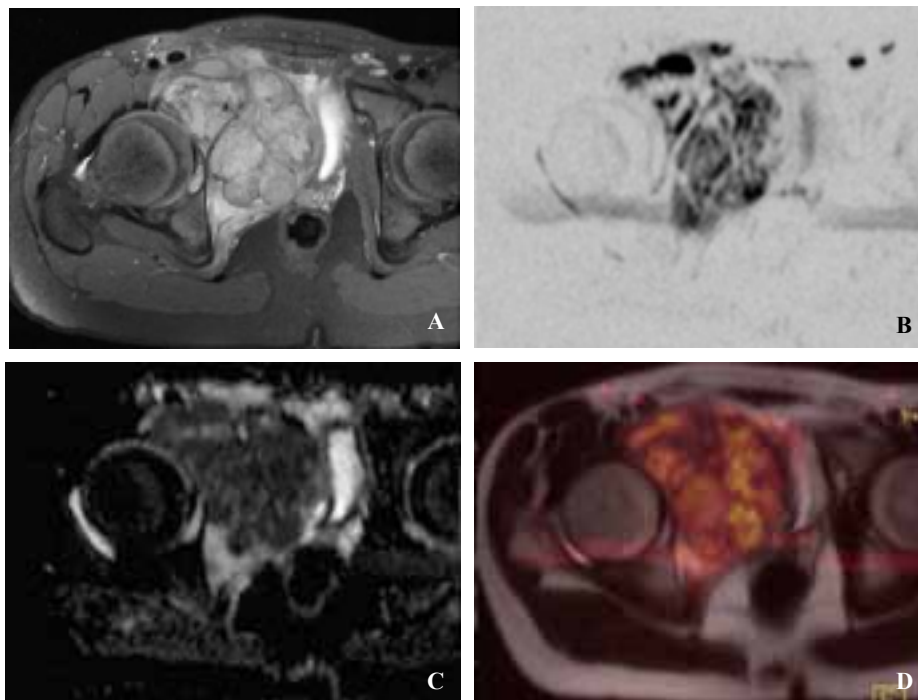
Fig. 1. Newly diagnosed Ewing's sarcoma in a 15-year-old boy. **A:** Contrast-enhanced T1w imaging with fat saturation shows a large tumor of the right pubic bone with destruction of the anterior acetabulum and infiltration of the pelvic floor; **B:** DWI with b=800 s/mm^2 and inverted gray-scale visualises highly restricted diffusion within the tumor; **C:** Mean ADC measured on the ADC map was 0.54×10^{-3} mm^2/s; **D:** Image fusion with colorized overlay of DWI b=800 s/mm^2 onto the T2 HASTE image produces a PET/MRI-like visual impression. ADC: apparent diffusion coefficient; DWI: diffusion-weighted imaging.
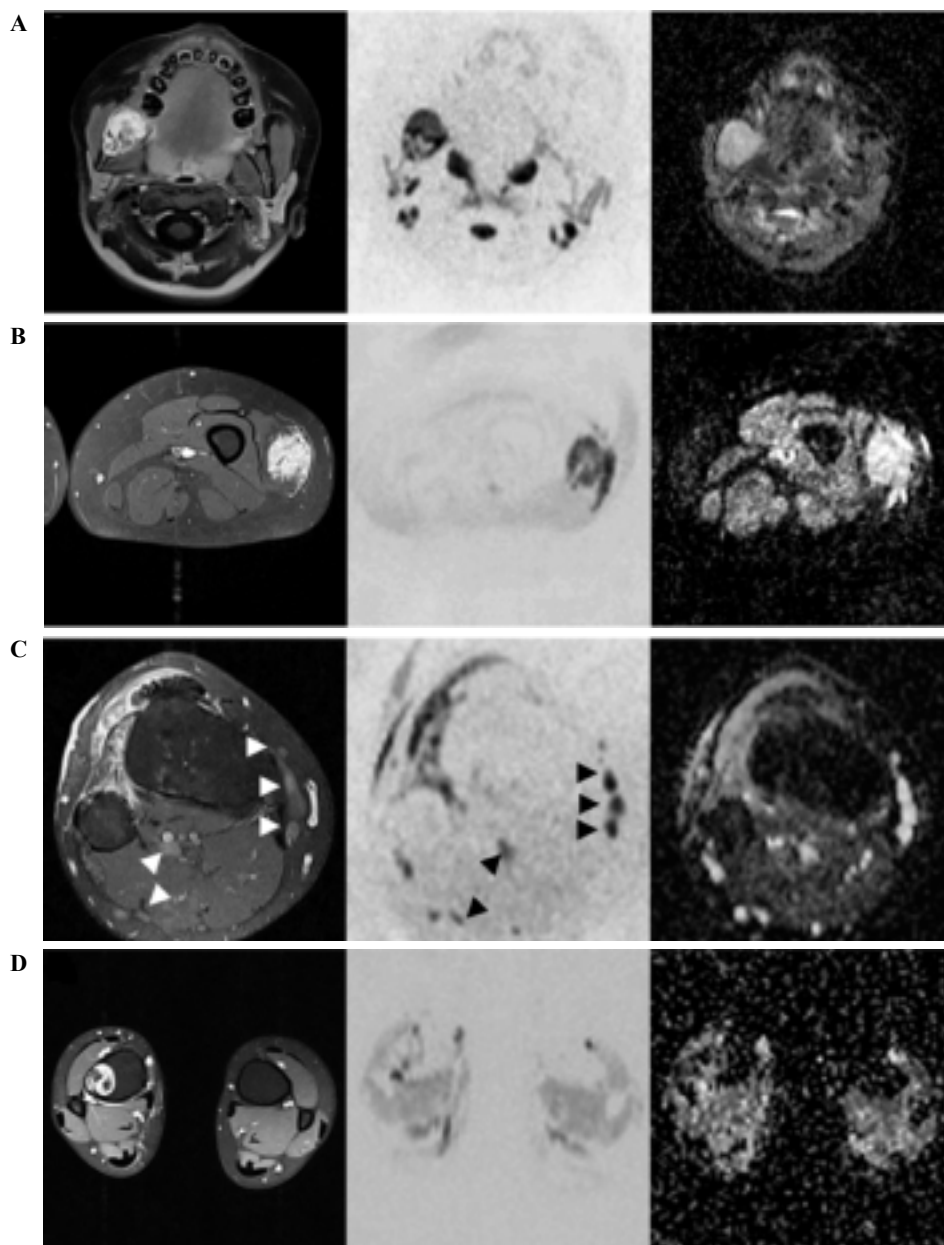
Fig. 2. A selection of benign lesions from our study group, presented as contrast-enhanced T1w imaging, DWI b=800 s/mm^2 and ADC map (left to right). **A:** Ameloblastic fibro-odontoma in the ramus of the right mandible in an 8-year-old boy (mean ADC=1.68×10^{-3} mm^2/s). The tumor showed matrix calcifications on CT and histology; **B:** Intramuscular hemangioma of the left vastus lateralis muscle in a 16-year-old girl (mean ADC=1.27×10^{-3} mm^2/s); **C:** Multiple small neurofibromas of the proximal lower leg in a 17-year-old female patient with known neurofibromatosis Recklinghausen. The neurofibromas (arrowheads) show a high signal on DWI due to a T2 shine-through artefact and a high mean ADC of 2.17×10^{-3} mm^2/s, but are hardly discernable on contrast-enhanced T1w imaging. A pretibial intramuscular hemangioma (mean ADC=1.59×10^{-3} mm^2/s) as a secondary finding; **D:** Non-ossifying fibroma of the distal tibia in a 15-year-old girl (mean ADC=1.8×10^{-3} mm^2/s). DWI: diffusion-weighted imaging; ADC: apparent diffusion coefficient.

was well-tolerated by all patients. Distortion artefacts were present on DWI in 6 of 17 patients with head and neck scans. One examination showed marked motion artefacts on ce-T1w, but not on DWI. All target lesions could be identified and measured on DWI and standard sequences.

Quantitative analysis

Variables of lesion size and mean ADC showed normal distribution (Kolmogorov-Smirnov test, $P>0.05$). Mean lesion size was 27±17 mm (range: 6-80 mm). No significant difference was observed in lesion size between measurement on DWI and on standard sequences (paired-samples t test, $P=0.926$).

Mean ADC was 0.78±0.45×10^{-3} mm^2/s (range: 0.42-1.98×10^{-3} mm^2/s) for malignant lesions and 1.72±0.75×10^{-3} mm^2/s (range: 0.58-4.28×10^{-3} mm^2/s) for benign ones ($P<0.001$). Among malignant lesions,
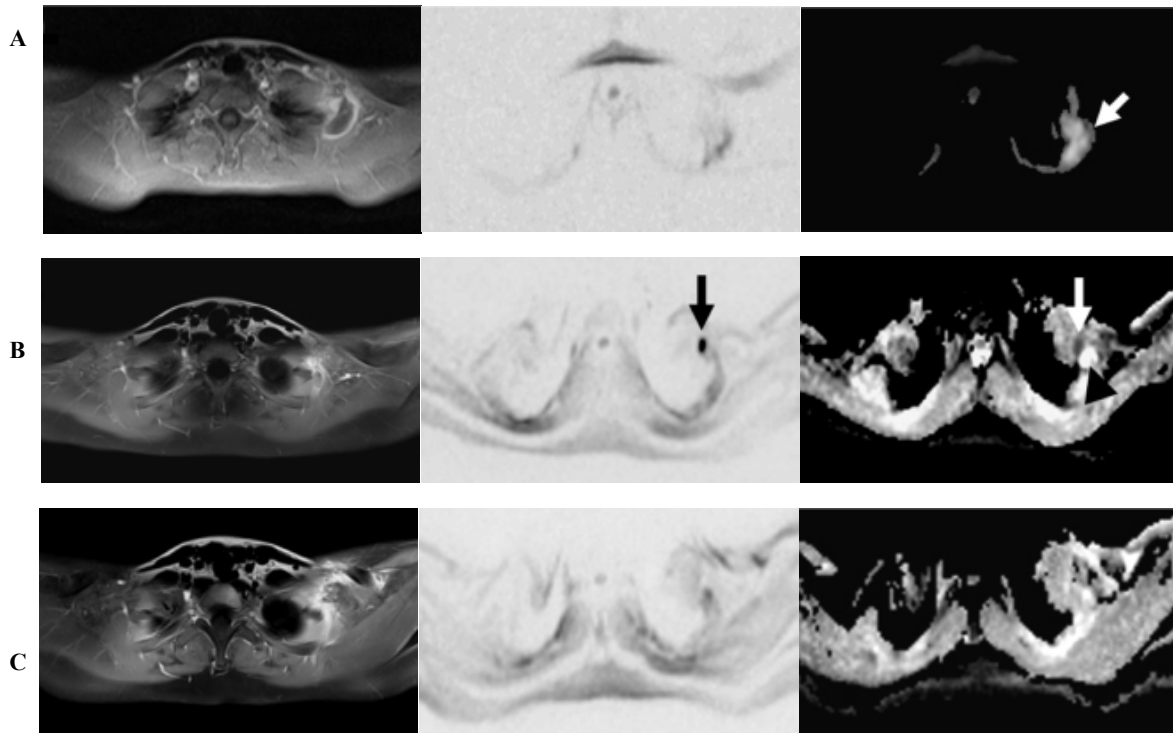
Fig. 3. MRI follow-up of synovial sarcoma in the left supraclavicular fossa (contrast-enhanced T1w, DWI b=800 s/mm^2, ADC map). A 16-year-old female patient was first referred to our institution two weeks after resection of a histologically proven synovial sarcoma with unclear status of resection margins. **A**: The initial examination showed postoperative seroma in the left supraclavicular fossa with a mean ADC of 2.91×10^{-3} mm^2/s (white arrow); **B**: On follow-up MRI 15 weeks post-operation, a tumor-suspicious lesion, 1.3×0.9 mm in transversal diameter, with nodular contrast enhancement, high focal signal on DWI and a mean ADC of 1.09×10^{-3} mm^2/s (arrow) was detected at the ventral margin of the resection site. Posteriorly adjacent residual seroma with low signal on DWI and mean ADC of 1.72×10^{-3} mm^2/s persisted (arrow head). The recurrent tumor was resected and confirmed histopathologically; **C**: MRI follow-up one month after completion of local radiotherapy showed strong regional contrast enhancement and edema in the absence of suspicious focal signal alterations on DWI. The lowest ADC measured at the surgical site was 1.51×10^{-3} mm^2/s. No sign of tumour recurrence was found on subsequent MRI over 15 months. DWI: diffusion-weighted imaging; ADC: apparent diffusion coefficient; MRI: magnetic resonance imaging.

Ewing sarcoma showed very low mean ADC with an average of 0.55×10^{-3} mm^2/s. The highest ADC values were seen in lymphangioma with a mean ADC of 3.29×10^{-3} mm^2/s. ADC showed no significant difference between benign lesions with or without subsequent biopsy (1.86±0.79 *vs.* 1.61±0.71×10^{-3} mm^2/s, *P*=0.362). Figs. 1, 2 demonstrate typical cases from our study cohort. In two patients, local recurrence of malignant tumors was diagnosed on DWI only (Fig. 3).

Malignant tumors were significantly larger than benign tumors (40±21 mm *vs.* 23±14 mm, *P*<0.001). Bivariate correlation analysis showed a positive correlation between lesion size and mean ADC for benign lesions (Pearson's correlation coefficient, *r*=0.41, *P*=0.017), but not for malignancies (*r*=−0.25, *P*=0.488).

Compared with post-contrast T1w imaging, DWI (b=800) showed higher signal intensity of tumor *vs.* surrounding soft tissue or bone marrow in malignant tumors (8.9 *vs.* 2.4, Wilcoxon's rank-sum test, *P*=0.002), but not in benign lesions (5.9 *vs.* 4.2, Wilcoxon's rank-sum test, *P*=0.168).

ROC and regression analysis

ROC analysis of mean ADC in malignant *vs.* benign lesions yielded an area under the curve of 0.89 (non-parametric assumption, standard error 0.074, *P*<0.001). Based on a cut-off value for mean ADC ≤1.03 ×10^{-3} mm^2/s, sensitivity and specificity for malignancy in our study group were 90% and 91%, respectively (Fig. 4). Discrimination of lesions using minimum or maximum ADC did not increase diagnostic performance.

On stepwise binary logistic regression modelling with tumour dignity as the dependent variable, low mean ADC and tumor size were both significant predictors of malignancy, accounting for 62% of the variation in dignity (Nagelkerke R square 0.62, correct classification 40 of 44, 91%, model *P*<0.001).

Mis-classified lesions

There was only one outlier among malignant tumors, which was a primitive myxoid sarcoma diagnosed in a two-month old girl with a mean ADC of 1.98×10^{-3} mm^2/s. Among the three benign lesions with a mean
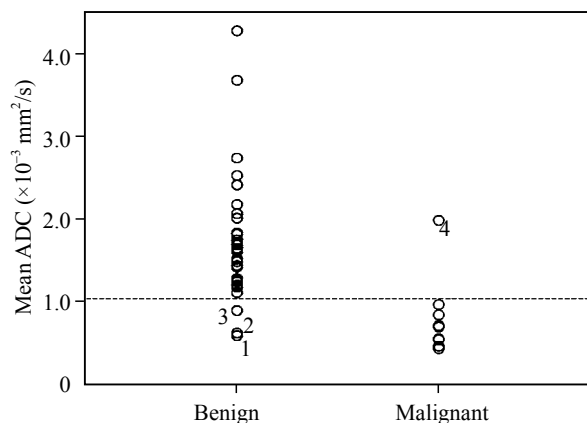
Fig. 4. Dot plot of mean ADC in benign and malignant lesions (one circle per lesion). The horizontal line marks the cut-off ADC value of 1.03×10^{-3} mm^2/s obtained from ROC analysis. Mis-classified lesions are marked as: 1 and 2, epidermoid; 3, non-ossifying fibroma; 4, primitive myxoid sarcoma. ADC: apparent diffusion coefficient; ROC: receiver operating characteristics.

ADC below the cut-off value, two cases of intraosseous epidermoid tumors of the skull were observed with a mean ADC of 0.58 and 0.61×10^{-3} mm^2/s. One case of non-ossifying fibroma, which measured 13 mm in diameter and appeared to be largely sclerotic with only a small contrast-enhancing soft tissue component, had a low ADC of 0.89×10^{-3} mm^2/s. None of the three patients with benign lesions was subjected to biopsy, as localization and imaging findings other than ADC were suggestive of benign disease.

Internal reference

Mean ADC measured in our patients as an internal reference across different MRI scanners was $0.79 \pm 0.08 \times 10^{-3}$ mm^2/s for pontine brain tissue (Avanto $n=6$, Symphony $n=10$), $2.85 \pm 0.09 \times 10^{-3}$ mm^2/s for the bulbus oculi (Avanto $n=5$, Symphony $n=10$), $1.17 \pm 0.12 \times 10^{-3}$ mm^2/s for skeletal muscle (Skyra $n=3$, Trio $n=1$, Avanto $n=11$, Symphony $n=3$) and $3.31 \pm 0.48 \times 10^{-3}$ mm^2/s for CSF (Skyra $n=1$, Avanto $n=5$, Symphony $n=16$) without significant differences between scanners.

Intra-observer variability was assessed with a second blinded reading by the same observer in 15 patients randomly chosen from our cohort. Coefficients of variation for lesion size on DWI, lesion size on ce-T1w and mean ADC were calculated as 8.6%, 10.9% and 8.1%, respectively.

Discussion

This study is the first to assess the use of DWI in evaluating the dignity of musculoskeletal tumorous lesions in a larger series of pediatric patients. The results of the study indicate high diagnostic accuracy of DWI, based on average ADC as a single parameter.

Clinically, musculoskeletal lesions in children present a wide spectrum of diseases, but most of them are benign. Many lesions are secondary findings on clinical examination or are incidentally discovered in imaging studies carried out for trauma or other causes. Malignant tumors of bone and soft tissue are less common, but present an important differential diagnosis. Stratification to some extent is based on clinical information about age, sex and course of symptoms. Certain tumor entities show typical features on multimodal diagnostic imaging in terms of localization, patterns of growth, and signal characteristics. In many cases, however, surgical biopsy is so far the only way to establish a diagnosis with confidence.[12] Imaging studies should help to guide invasive diagnostic measures and limit the proportion of patients with benign disease who undergo biopsy.

DWI is a novel approach to tissue differentiation, which has shown promising results in musculoskeletal lesions among adult patients,[13] but limited data are available for pediatric patients. Targeted regional DWI with a small scan volume for lesion characterisation required little extra scanning time of less than 3 minutes with a small FOV at 1.5 Tesla in our study, but more extensive volume coverage significantly added scan time to the examination protocol. All lesions were visualized without significant difference in tumor size on both DWI and ce-T1w. DWI based on echo planar imaging (EPI) is prone to distortion artefacts secondary to B0 field inhomogenities, which are most frequently observed in the head and neck region[14] and distal extremities. Such artefacts were also present in about one-third of our patients undergoing a head and neck DWI scan without compromise to diagnostic image quality. Diffusion-weighted EPI which is relatively insensitive to bulk motion artefacts facilitated image acquisition of the trunk in free-breathing mode and minimized motion artefacts. Compared with ce-T1w, DWI showed superior signal intensity ratios in malignant tumors, but there was no significant difference in benign lesions. Therefore, DWI with high b-values aids the detection of malignant tumors by high signal intensity without the need of intravenous contrast and by suppression of the anatomical background. We found that DWI is feasible in children and may be considered particularly suitable for pediatric patients, in whom compliance with breath-hold techniques, patient motions and placement of peripheral intravenous lines are of concern. The cut-off value for mean ADC ($\leq 1.03 \times 10^{-3}$ mm^2/s) from ROC analysis in our study corresponded well to the results from previous studies

Original article

on head and neck tumors[14] and malignant bone tumors in children.[9,15]

The only false-negative malignant tumor in our study group was a cervical primitive myxoid sarcoma in a two-month old girl. The tumor was initially considered a vascular lesion on MRI for its high T2w signal intensity, strong contrast enhancement and high ADC approaching 2×10^{-3} mm²/s. Correct diagnosis was established with surgical biopsy performed after tumor progression on MRI follow-up. High ADC was demonstrated in myxoid malignant tumors or mucinous carcinoma of the breast on MR mammography[16] and also in malignant and benign myxoid soft tissue tumors.[17,18] Our patients underwent VAC chemotherapy (vincristine, actinomycin D, cyclophosphamide), which resulted in a fulminant progress with a doubled diameter and a concomitant significant drop in mean ADC from 1.98×10^{-3} to 1.60×10^{-3} mm²/s. Surgical tumor reduction was attempted, but after the reduction, tumor ADC remained unchanged. Radiation therapy achieved local tumor control with partial remission and an increase of ADC to 2.0×10^{-3} mm²/s in the residual tumor tissue.

Two small well-defined intraosseous lesions of the skull exhibiting very low ADC values of 0.58 and 0.61×10^{-3} mm²/s were diagnosed as epidermoid tumors in our study. Strongly restricted diffusion in intracranial epidermoids is a classical finding in neuroimaging, and intraosseous lesions appear to show similar signal characteristics. A third benign lesion with ADC $\leq1.0\times10^{-3}$ mm²/s was a non-ossifying fibroma with a total transversal diameter of 13 mm, which was largely sclerotic and had only a tiny contrast-enhancing soft tissue component. The significant positive correlation between ADC and size in benign lesions and the smaller size of these lesions, compared to malignant neoplasm, suggests that partial volume effects may cause false-low ADC measurements in small target lesions compared to the spatial resolution of DWI. Therefore, ADC values measured in small tumors need to be interpreted with care. In general, diagnostic projections regarding tumor dignity should not depend on a single imaging parameter. In routine imaging, DWI and ADC need to be interpreted within the context of findings from standard MRI sequences, other imaging modalities and clinical data.

Limitations

The patients were examined with different MR scanners at two different field strengths. About 60% of all examinations, however, were performed on a 1.5 Tesla Magnetom Symphony; therefore, our findings should be reproducible with such equipment. The other scanners provide better scanning performance and superior image quality, and particularly so for DWI. The scan protocols were implemented on each scanner with consideration for consistency. Comparison of ADC of reference tissues did not show any significant differences between scanners. To our experience, variation in ADC mostly arises from subjective factors, such as ROI placement, while differences in scanner hardware appear to be less important, provided that basic scanning parameters are consistently chosen. Analysis of our internal reference values indicate that, in general, ADC measurements do compare well between different scanner hardwares of the same manufacturer. We suggest that DWI studies should include ADC values of internal reference tissues to facilitate between-studies comparability.

We acquired all DWI studies with transversal orientation, even though in some patients coronal or sagittal cross-sections would have been more appropriate from a diagnostic point of view. To our experience, SS-EPI DWI scans are limited to transversal cross-sections with the 1.5 Tesla Magnetom Symphony in order to control distortion artefacts. Coronal, sagittal or angled acquisition frequently suffer from severe distortion most pronounced at the extremities, not amendable with manual shimming, and cause DWI studies to yield non-diagnostic image quality. We therefore uniformly acquired transversal DWI for our study as well as for clinical routine.

The relatively low spatial resolution used in our study presents a compromise to get sufficient signal within reasonable scanning time. As the majority of musculoskeletal lesions referred to MRI for further diagnostic work-up would be relatively large, compared to the scan resolution, the scanning parameters may be sufficient for lesion detection. Quantitative analysis of small lesions on ADC maps, however, may be influenced by partial volume effects with a bias towards lower ADC values, thus inviting false-positive findings.

For analysis of signal intensity ratios, we chose a common reference standard to accommodate both osseous and soft tissue tumors (i.e. contrast-enhanced T1w) for standard MRI. Osseous lesions sometimes show better delineation on native T1w images, while measuring signal intensity of soft tissue tumors on such sequences is of little practical use. Furthermore, some bone tumors such as non-ossifying fibroma show generally low signal intensity on native T1w, while the contrast-enhancing (fibrotic) portions of the tumor correspond to the high signal intensity on DWI. Therefore, we decided to uniformly compare contrast-enhanced T1w imaging with DWI in all tumorous lesions, although other standard sequences may have shown better detectability and signal intensity for some lesions. Tumoral contrast enhancement was assessed on post-contrast T1w images with fat saturation. For

neuroimaging and in adult patients, we have successfully used subtraction techniques with pre- and post-contrast T1w sequences. In children, motion occurred more frequently between the scans, occasionally in response to intravenous contrast, and in our experience it degraded the quality of subtraction images. We therefore routinely perform post-contrast T1w scans with fat saturation in children and attempt subtraction in patients with insufficient fat saturation only.

Finally, an issue that should be considered is the spectrum of pathologies included in the study. This study aimed to assess whether DWI can distinguish between malignant and benign musculoskeletal tumors in a pediatric cohort referred to MRI. The series of consecutive patients in this study therefore present with a wide spectrum of lesions, which are both strength and weakness. Imaging features of certain tumor entities as a potentially interesting aspect cannot be deducted from our study.

In summary, we consider DWI an innovative imaging technique for characterisation of musculoskeletal lesions, which is particularly suitable for pediatric patients. DWI with large volume coverage may facilitate more reliable detection of musculoskeletal tumors for its merits of anatomical background suppression and superior signal intensity in malignant tumors. The earlier detectability of local tumor recurrence in postoperative scar tissue warrants further evaluation in controlled studies. Employed as a supplement to routine MRI sequences, DWI can be expected to aid decision-making to perform or to postpone biopsy with higher diagnostic confidence. DWI may therefore be of particular value to avoid invasive diagnostic procedures in benign pathologies.

References

1　De Schepper AM, De Beuckeleer L, Vandevenne J, Somville J. Magnetic resonance imaging of soft tissue tumors. Eur Radiol 2000;10:213-223.
2　Shapeero LG, Vanel D, Verstraete KL, Bloem JL. Fast magnetic resonance imaging with contrast for soft tissue sarcoma viability. Clin Orthop 2002:212-227.
3　Moulton JS, Blebea JS, Dunco DM, Braley SE, Bisset GS 3rd, Emery KH. MR imaging of soft-tissue masses: diagnostic efficacy and value of distinguishing between benign and malignant lesions. AJR Am J Roentgenol 1995;164:1191-1199.
4　Daniel A Jr, Ullah E, Wahab S, Kumar V Jr. Relevance of MRI in prediction of malignancy of musculoskeletal system- A prospective evaluation. BMC Musculoskelet Disord 2009;10:125.
5　Balzarini L, Sicilia A, Ceglia E, Tesoro Tess JD, Trecate G, Musumeci R. Magnetic resonance in primary bone tumors: a review of 10 years of activities. Radiol Med (Torino) 1996;91:344-347.
6　Bley TA, Wieben O, Uhl M. Diffusion-weighted MR imaging in musculoskeletal radiology: applications in trauma, tumors, and inflammation. Magn Reson Imaging Clin N Am 2009;17:263-275.
7　Baur A, Reiser MF. Diffusion-weighted imaging of the musculoskeletal system in humans. Skeletal Radiol 2000;29:555-562.
8　van Rijswijk CS, Kunz P, Hogendoorn PC, Taminiau AH, Doornbos J, Bloem JL. Diffusion-weighted MRI in the characterization of soft-tissue tumors. J Magn Reson Imaging 2002;15:302-307.
9　Oka K, Yakushiji T, Sato H, Fujimoto T, Hirai T, Yamashita Y, et al. Usefulness of diffusion-weighted imaging for differentiating between desmoid tumors and malignant soft tissue tumors. J Magn Reson Imaging 2011;33:189-193.
10　Uhl M, Saueressig U, Koehler G, Kontny U, Niemeyer C, Reichardt W, et al. Evaluation of tumour necrosis during chemotherapy with diffusion-weighted MR imaging: preliminary results in osteosarcomas. Pediatr Radiol 2006;36:1306-1311.
11　Hayashida Y, Yakushiji T, Awai K, Katahira K, Nakayama Y, Shimomura O, et al. Monitoring therapeutic responses of primary bone tumors by diffusion-weighted image: initial results. Eur Radiol 2006;16:2637-2643.
12　Meuwly J, Lepori D, Theumann N, Schnyder P, Etechami G, Hohlfeld J, et al. Multimodality imaging evaluation of the pediatric neck: techniques and spectrum of findings. Radiographics 2005;25:931-948.
13　Costa FM, Ferreira EC, Vianna EM. Diffusion-weighted magnetic resonance imaging for the evaluation of musculoskeletal tumors. Magn Reson Imaging Clin N Am 2011;19:159-180.
14　Abdel Razek AA, Gaballa G, Elhawarey G, Megahed AS, Hafez M, Nada N. Characterization of pediatric head and neck masses with diffusion-weighted MR imaging. Eur Radiol 2009;19:201-208.
15　Oka K, Yakushiji T, Sato H, Hirai T, Yamashita Y, Mizuta H. The value of diffusion-weighted imaging for monitoring the chemotherapeutic response of osteosarcoma: a comparison between average apparent diffusion coefficient and minimum apparent diffusion coefficient. Skeletal Radiol 2010;39:141-146.
16　Woodhams R, Kakita S, Hata H, Iwabuchi k, Umeoka S, Mountford CE, et al. Diffusion-weighted Imaging of mucinous carcinoma of the breast: evaluation of apparent diffusion coefficient and signal intensity in correlation with histologic findings. AJR Am J Roentgenol 2009;193:260-266.
17　Nagata S, Nishimura H, Uchida M, Sakoda J, Tonan T, Hiraoka K, et al. Diffusion-weighted imaging of soft tissue tumors: usefulness of the apparent diffusion coefficient for differential diagnosis. Radiat Med 2008;26:287-295.
18　Einarsdottir H, Karlsson M, Wejde J, Bauer HC. Diffusion-weighted MRI of soft tissue tumours. Eur Radiol 2004;14:959-963.

Original article